Prediction and Measurement of Thermal Residual Stresses in AA2024-T3 Friction Stir Welds

L. Dubourg,[1] P. Doran,[1] S. Larose,[1] M. A. Gharghouri,[2] and M. Jahazi[1]

[1] Aerospace Manufacturing Technology Centre, National Research Council Canada, Montreal, Canada, H3T 2B2

[2] Canadian Neutron Beam Centre, National Research Council, Chalk River Laboratories, Chalk River, On, Canada K0J 1J0

Friction stir welding (FSW) is an emerging manufacturing technology increasingly used in the aerospace industry. The National Research Council Canada's Institute for Aerospace Research has undertaken a major initiative to manufacture a fuselage panel using FSW. This multipronged study includes structural design, process optimization, evaluation of mechanical properties, NDE and robotic processing. Aircraft fuselage panels are usually composed of stringers and frames riveted onto a skin. For this application, FSW was an interesting alternative to rivets for creating lighter and more aerodynamic structures at lower cost [1,2]. However, stringer to skin joints pose a significant problem because of panel distortion [2,3]. The aim of the present work was to model the influence of friction stir welding parameters on the residual stresses, using a thermo-mechanical simulation developed using LS-DYNA finite element software.

Friction stir welds were made using a MTS I-STIR machine operated in position control welding mode using standard FSW tools made of H13 tool steel. 2.3-mm thick 2024-T3 plate was used for these tests. The influence of travelling speed (2, 6 and 10 mm/s) and rotational speed (500, 1000 and 1500 RPM) was investigated. All other welding parameters were kept constant. Thermocouples attached to the aluminum plate were used to monitor temperature during welding. The aluminum plate was clamped to a stainless steel backing anvil to prevent distortion during welding.

Residual lattice strains were measured by neutron diffraction using the L3 strain-scanning spectrometer. The aluminum plate remained clamped to the backing anvil for these measurements. Lattice strains were measured parallel to the longitudinal (parallel to the weld), normal (perpendicular to the Al plate surface), and transverse directions, at the middle length of the weld. This allowed us to determine the corresponding residual stresses. A sampling volume of 2 x 2 x (2-20) mm^3 was used, depending on the component of strain being measured. Different stress-free scattering angles ($2\theta_0$), acquired from small coupons extracted from a component after all the measurements were done, were used for the weld and base material.

A finite element model was developed using LS-DYNA to study the thermal cycles and induced stresses that occur during FSW. The model takes into account the temperature-dependent mechanical and thermophysical properties of the base material. As a first step, the thermal history was predicted considering tool friction as a heat source, an approach which has been used successfully elsewhere [4,5]. The model was calibrated using an inverse method based on temperature measurements at various locations close to the weld centreline [4,5]. The temperature distribution generated by the thermal model was then sequentially coupled to a mechanical model to predict the residual stresses.

The model dimensions of the aluminum plate and backing anvil were respectively 140 x 100 x 2.3 mm^3 and 140 x 100 x 12 mm^3. The mesh was refined in the vicinity of the welding tool. Heat flow was treated as a pure heat conduction problem, ignoring material flow around the FSW tool. Heating was modelled as a surface heat generation term and related to the basic welding process parameters via equation 1, where q is the surface heat flux (W/m2), ω is the rotational speed of the tool (rad/s), M is the welding torque recorded by the welding machine, r is the radius of the tool shoulder and η is a process efficiency that takes into account the heat lost to the welding tool.

$$q = \eta \frac{\omega \times M}{\pi \times r^2} \quad (1)$$

All nodes had an initial temperature of 23°C. The heat source was located at the bottom surface of the welding tool and moved along the weld line at the travelling speed. Convection was found to have a negligible effect on the predicted temperature distribution, so was excluded from the model. Radiation heat loss was also neglected. Two different heat transfer coefficients were defined for the model: H for high-pressure contact under the FSW tool and H0 for low-pressure contact under the rest of the plate. H was larger than $H0$ in order to take into account the improved contact between the Al plate and the backing anvil due to tool pressure. η, H, and $H0$ were calibrated using an inverse method based on temperature measurements as a function of rotational speed. The process efficiency decreased with increasing rotational speed, due to the increase in tool temperature with rotational speed. For the mechanical analysis, the FSW tool and the backing anvil were treated as rigid contact surfaces. To simulate the effect of the clamping device, all displacement and rotational degrees of freedom were blocked along the longitudinal edge of the plate. After tool motion was done, the simulation was allowed to continue until the Al plate cooled down to allow the residual stresses to develop. The release phase from the clamping device was thus *not* simulated, such that the predicted and measured stresses reported correspond to those before the clamping pressure was released.

Results for a weld performed with a tool rotational speed of 1000 RPM, and a travelling speed of 6 $mm.s^{-1}$ are presented here. The measured and predicted temperatures as a function of distance from the weld centreline are compared in Figure 1. The differences are negligible, but the predicted temperature

profile shows an unrealistic plateau of about 350°C in the weld (where no measurements were made). This is likely a consequence of modeling the heat generated by the FSW tool as a constant heat flux, which yields a top-hat heating profile. The assumption here is that material flow around the tool tends to homogenize the temperature under the FSW tool. However, a Gaussian temperature profile may be more appropriate.

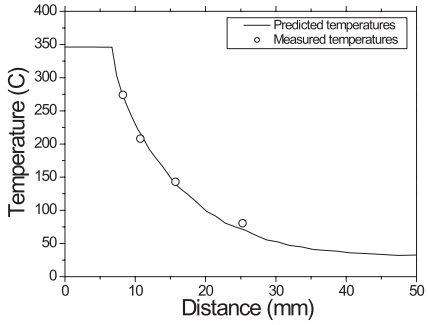

Fig 1. *Measured and predicted temperatures as a function of distance from the weld centreline.*

The measured and predicted longitudinal and transverse residual stresses are shown in Figs. 2(a) and (b), respectively. The results are plotted as a function of distance from the weld centreline.

Regarding the longitudinal stresses in Fig. 2(a), an acceptable match is observed: the predicted and measured profiles show tensile stresses close to the yield strength of 2024-T3 base metal (345 MPa) in the weld area and compressive stresses in the rest of the plate. This tendency agrees with many previous investigations [4, 6-8]. However, the predicted tensile stresses in the weld are higher than the measured ones. It can also be seen that the predicted stress gradient is sharper than that revealed by neutron diffraction.

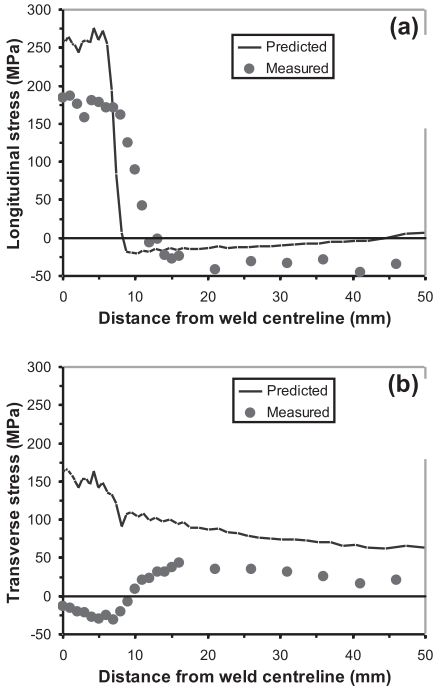

Fig 2. *Measured and predicted residual stresses: (a) longitudinal stresses, (b) transverse stresses.*

The predicted and measured trends in the base metal are somewhat different (Figure 2(b)). The predicted stresses are most negative close to the weld, becoming progressively more tensile further away from the weld. Conversely, the measured stresses remain constant beyond a distance of approximately 20 mm from the weld centreline. These differences could be explained by the lack of blocked nodes close to the heating zone simulating the effects of the clamping device.

In the transverse direction, modelled and measured stresses were tensile in the base metal, similar results having been reported in [4, 6-8]. However, the predicted and measured profiles diverge significantly in the weld zone, where the measured stresses are weakly compressive while the predicted stresses are strongly tensile. This difference may be due to the presence of blocked nodes at the edge of the Al plate, which prevented plate expansion along the transverse direction, thereby distorting the predicted build-up of residual stresses.

This study highlighted the following points. i) The difference between the predicted and measured temperatures was negligible. This confirmed the relevance of the inverse method for calibrating the thermal model and the usage of the two different heat transfer coefficients between the Al plate and the backing anvil. The heat transfer coefficient under the FSW tool was higher than for the rest of the plate in order to take into account the better contact due to tool pressure. ii) The predicted longitudinal residual stresses are in good agreement with the measurements performed by neutron diffraction validating the model assumptions: no material flow around the FSW tool and a top hat profile of the heating source. However, improvements should be brought in the mechanical analysis to take into account a more realistic clamping situation.

Acknowledgements

The authors thank A. Baudoin and M. Guerin for welding experiments and thermocouple recording.

References

[1] B. Christner, J. Mc Coury, S. Higgins, in: 4th International Symposium on Friction Stir Welding, Park City, UT, USA, May14-16, TWI Ltd, Abington, Cambridge CB1 6AL, UK (2003).
[2] A. Murphy, M. Price, P. Wang, in: 46th AIAA/ASME/ASCE/AHS/ASC Structures, Structural Dynamics, and Materials Conference, Austin, TX, USA, pp 1-15, April 18-21 (2005).
[3] P. Michaleris, X. Sun, Welding Journal, 76 (11), pp. 451-s-457-s (1997).
[4] Z. M. Hu, P. B. J. W. Brooks, Residual Stresses in Friction Stir Welding, in: 2004 ABAQUS Users' Conference (2004).
[5] T. De Vuyst, L. D'Alvise, A. Simar, B. De Meester, S. Pierret, Welding in the World, 49 (3-4), pp. 47-55 (2005).
[6] H. W. Zhang, Z. Zhang, J. T. Chen, Materials Science and Engineering A, 403 (1-2), pp. 340-348 (2005).
[7] M. Prime, T. Gnaupel Herold, J. Baumann, R. Lederich, D. Bowden, R. Sebring, Acta Materialia, 54 (15), pp. 4013-4021 (2006).
[8] M. H. Khandkar, J. Khan, A. P. Reynolds, M. A. Sutton, Journal of Materials Processing Technology, 174 (1-3), pp. 195-203 (2006).